

Design considerations for the free-electron laser with the self-seeding and current-enhanced SASE¹

Alexander Zholents

*Advanced Photon Source, Argonne National Laboratory
Argonne, IL 60439*

The submitted manuscript has been created by UChicago Argonne, LLC, Operator of Argonne National Laboratory ("Argonne"). Argonne, a U.S. Department of Energy Office of Science laboratory, is operated under Contract No. DE-AC02-06CH11357. The U.S. Government retains for itself, and others acting on its behalf, a paid-up nonexclusive, irrevocable worldwide license in said article to reproduce, prepare derivative works, distribute copies to the public, and perform publicly and display publicly, by or on behalf of the Government.

To be published as a Light Source Technical Notes

¹Work supported by the U. S. Department of Energy, Office of Science, under Contract No. DE-AC02-06CH11357.

Design considerations for the free-electron laser with the self-seeding and current-enhanced SASE

NGLS Technical Note 46

Alexander Zholents
Argonne National Laboratory
6 August 2013

Table of Contents

I. Introduction	4
II. Undulator magnetic field.	4
III. Electron Beam Energy	5
IV. FEL performance using ESASE	8
V. Conclusion	12
VI. References:	13

I. Introduction

Cost of the facility producing x-rays using free-electron lasers (FELs) is largely defined by the electron beam energy E_0 and by the availability of the undulators with a certain period that will support production of photons in the range of photon energies between $\hbar\omega_1$ and $\hbar\omega_2$ corresponding to the wavelengths λ_1 and λ_2 . Here we first consider a trade-off of various parameters that could provide initial guidance in the cost optimization of the FEL covering the range of photon energies from $\hbar\omega_1 = 4$ keV to $\hbar\omega_2 = 5$ keV. In this analysis we also compare helical and planar undulators. After selecting a preferred set of parameters, we proceed with a preliminary design of the FEL that employs self-seeding and enhanced SASE techniques.

II. Undulator Magnetic Field

A superconducting undulator seems to be the best undulator choice for the FEL optimized to produce photons with the highest energy with the minimal energy electron beam. Recent progress in the development and construction of the superconducting undulators [1] confirmed their superior performance. Thus, here we consider an undulator based on Nb₃Sn wire that according to Ref. [2] can produce the following peak magnetic field:

$$B = ae^{b(g/\lambda_u)+c(g/\lambda_u)^2+d(g/\lambda_u)^3} \quad (1)$$

where λ_u is an undulator period, g is an undulator gap, and coefficients a , b , c , d are given in Table 1 for the helical and planar undulator configurations [3]:

Table 1

Undulator type	a	b	c	d
Helical	119.934 kG	-3.7977	0.3364	0.0
Planar	220.091 kG	-9.0877	7.9639	-3.5986

Figure 1 shows B as a function of the ratio g/λ_u calculated using Eq. (1) and Table 1.

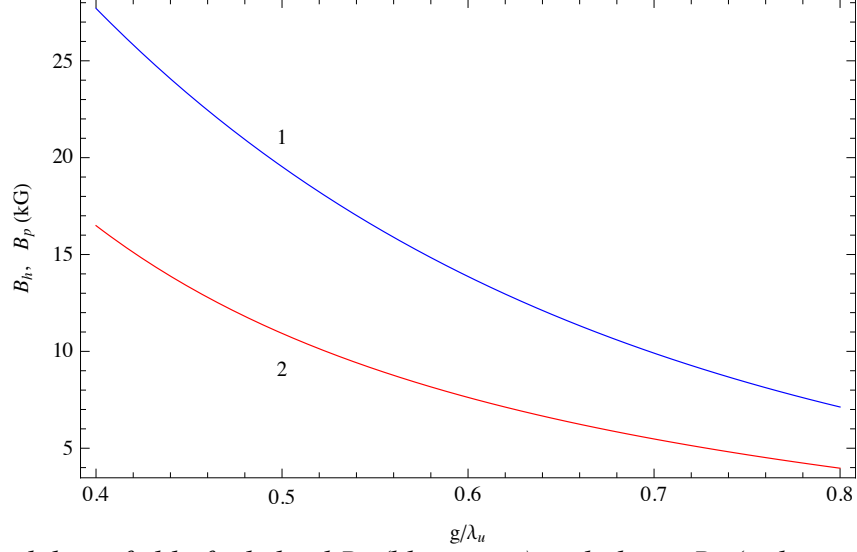


Fig. 1. Peak undulator field of a helical B_h (blue curve) and planar B_p (red curve) undulators as a function of the ratio g / λ_u .

III. Electron Beam Energy

Another figure of merit of undulator performance is the undulator parameter $K = \frac{eB\lambda_u}{2\pi mc}$, where

m and e are the electron mass and charge, respectively, and c is the speed of light. Although we use the same notation for the coefficient c in Eq. (1) and for the speed of light, the specific use of c is obvious from its context in each case. The wavelength of the undulator radiation with helical and planar polarization is equal to:

$$\text{Helical:} \quad \lambda = \frac{\lambda_u}{2\gamma^2} (1 + K^2) \quad (2)$$

$$\text{Planar:} \quad \lambda = \frac{\lambda_u}{2\gamma^2} (1 + K^2 / 2)$$

We note that the field (and, therefore, the undulator parameter K) is smaller for a larger g / λ_u . Although, it is good to have a large undulator field, we may nevertheless prefer a relatively small λ_u and a large g for the following reason. Our goal is to provide x-rays at the shortest wavelength using the lowest possible electron beam energy; for this case it helps to have a small λ_u , according to Eq. (2).

Now, consider an FEL producing light in the range of wavelengths from λ_1 to λ_2 . According to Eq. (2), one can use γ and K to vary the wavelength. However, using γ may not be convenient when more than one FEL shares the same electron beam accelerator. Therefore, we assume that it will be done through changing K by adjusting the magnetic field. In this case we can write:

Helical:
$$K_2 = \sqrt{\frac{\lambda_2 - \lambda_1}{\lambda_1} (1 + K_1^2) + K_1^2}, \quad (3)$$

Planar:
$$K_2 = \sqrt{\frac{\lambda_2 - \lambda_1}{\lambda_1} (2 + K_1^2) + K_1^2},$$

where $K_2 > K_1$ is the undulator parameter for the longer wavelength λ_2 , and K_1 is the undulator parameter for the shorter wavelength λ_1 . In Figure 2 we plot the FEL Pierce parameter ρ [4] as a function of K for a helical and planar undulator assuming at this point the following specific beam parameters: normalized emittance of 0.6 μm , an average beta function in the undulator of 10 m, an electron peak current of 500 A, and an electron beam energy of 3 GeV. From this plot one can see that ρ -values at the 90% levels of the peaks can be achieved in the case of a helical undulator with $K_1 = 0.562$ and in the case of a planar undulator with $K_1 = 0.685$.

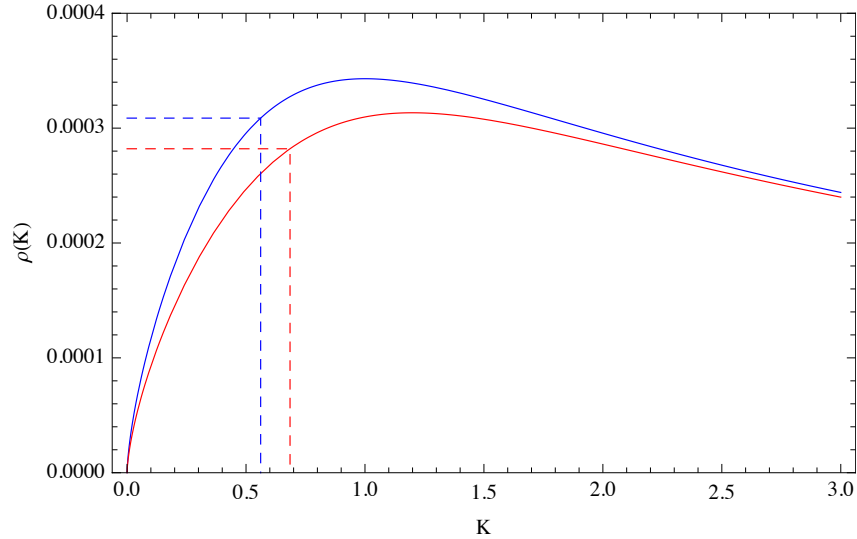


Fig. 2. The Pierce parameters as a function of K for the helical undulator (blue curve) and for the planar undulator (red curve) calculated for the beam parameters indicated in the text. Dotted lines show K values at the levels of 90% of peaks.

For brevity, we describe next few steps in the analysis only for the helical undulator. They are very similar for a planar undulator, although exact expressions are somewhat longer.

Using Eqs. (1) and (3), we write:

$$\sqrt{\frac{\lambda_2 - \lambda_1}{\lambda_1} (1 + K_1^2) + K_1^2} = \frac{e\lambda_u}{2\pi mc} a e^{b(g/\lambda_u) + c(g/\lambda_u)^2 + d(g/\lambda_u)^3} \quad (4)$$

Next, using 4 keV and 5 keV for the photon energy range we calculate $\frac{\lambda_2 - \lambda_1}{\lambda_1} = 0.25$ and using $K_1 = 0.562$ (as indicated in Fig. 4), we obtain from Eq. (4):

$$g = 10 \frac{\lambda_u}{[cm/mm]} \left[5.6446 - 1.4863 \sqrt{10.87 - 13.46 \text{Log} \left(\frac{\lambda_u}{[cm]} \right)} \right], \quad (5)$$

where g is measured in mm, and λ_u is measured in cm. We tabulate Eq. (5) and fit the result with a quadratic polynomial to find λ_u as a function of g :

$$\lambda_u = 0.2852 + \frac{0.09947}{[mm/cm]} g - \frac{0.00051}{[mm/cm]^2} g^2 \quad (6)$$

The initial data and the fit are shown in Fig. 3 for both helical and planar undulators. (Note that for the planar undulator we used $K_1 = 0.685$.)

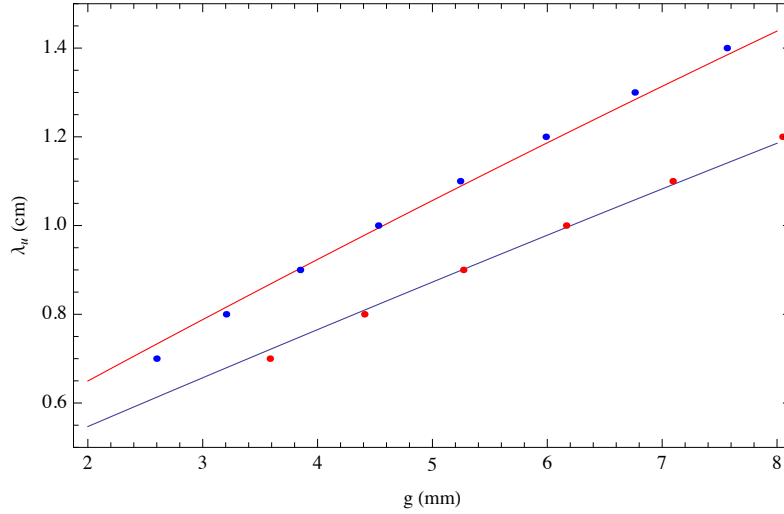


Fig. 3. The undulator period λ_u as a function of the magnetic gap g . Initial data are shown with dots, and the fit is shown with a solid line: helical undulator (blue line and red dots) and planar undulator (red line and blue dots).

Finally we use in Eq. (2) the above-defined function $\lambda_u(g)$ and $K \equiv K_2$ from Eq. (3) and obtain the minimum electron beam energy required for production of x-rays within the range of wavelengths from λ_1 to λ_2 as a function of the magnetic gap g :

$$\text{Helical:} \quad E = mc^2 \sqrt{\frac{\lambda_u(g)}{2\lambda_2} \left(1 + \frac{\lambda_2 - \lambda_1}{\lambda_1} (1 + K_1^2) + K_1^2 \right)}, \quad (7)$$

$$\text{Planar:} \quad E = mc^2 \sqrt{\frac{\lambda_u(g)}{2\lambda_2} \left(1 + \frac{\lambda_2 - \lambda_1}{\lambda_1} (1 + K_1^2 / 2) + K_1^2 / 2 \right)},$$

where $K_1 = 0.562$ for helical and $K_1 = 0.685$ for planar undulators as defined above. Figure 4 shows a minimum E as a function of g calculated for $\lambda_1 = 3.1 \text{ \AA}$ to $\lambda_2 = 2.5 \text{ \AA}$. Dots show calculations using Eq. (8), and the line shows the fit with a quadratic polynomial:

Helical:
$$E(\text{GeV}) = 1.4576 + \frac{0.1970}{[\text{mm}]} g - \frac{0.0053}{[\text{mm}^2]} g^2, \quad (8)$$

Planar:
$$E(\text{GeV}) = 1.7213 + \frac{0.2529}{[\text{mm}]} g - \frac{0.0076}{[\text{mm}^2]} g^2.$$

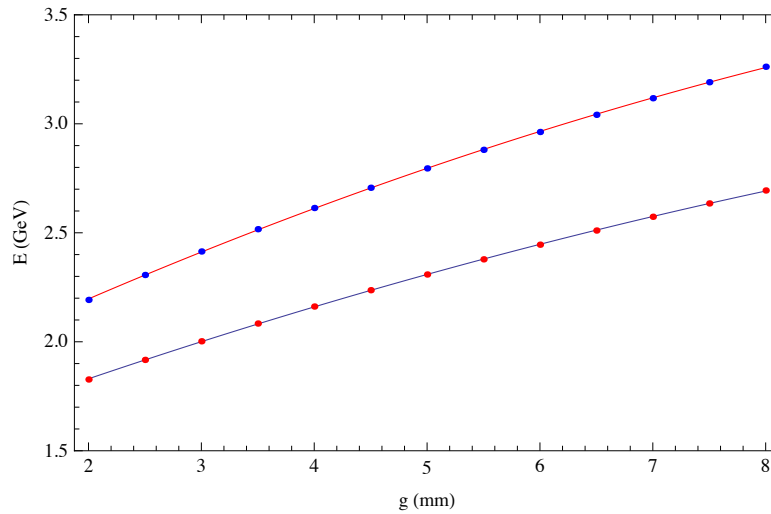


Fig. 4. The minimum electron beam energy required for production of x-rays within the range of photon energies from 4 keV to 5 keV as a function of the magnetic gap g for a helical undulator (blue curve and red dots) and a planar undulator (red curve and blue dots).

Summarizing this paragraph, we collect several specific examples in Table 2.

Table 2

Undulator type	g , mm	λ_u , cm	E , GeV
Helical	6	0.86	2.45
	7	0.96	2.57
Planar	6	1.19	2.97
	7	1.31	3.12

IV. FEL Performance Using Current Enhanced SASE

Based on the above analysis we now continue with the FEL design using the two types of undulators listed in Table 3. Note that the corresponding electron beam energy in each case in Table 3 is higher by 10% comparing to the minimal required beam energy listed in Table 2. This is used as a bit arbitrary “safety” factor.

Table 3

Undulator type	Magnetic gap	Period	Beam energy
Helical	6 mm	0.9 cm	2.7 GeV
Planar	6 mm	1.2 cm	3.3 GeV

The other electron beam parameters are given in Table 4.

Table 4

Bunch charge, Q	300 pC
Peak current, I_0 (flat distribution)	500 A
Normalized emittance, ε_n	0.6 μm
Energy spread, σ_E	150 keV
Average beta function, β (in the undulator)	10 m

Using these parameters and the Ming-Xie algorithm [5], we calculate a 3D FEL power gain length as a function of the electron peak current. Each new value of the peak current was accompanied with the correspondent increase of the energy spread, i.e., $\sigma_E \sim I/I_0$. The result is plotted in Figure 5. Note the intensity gain length is two times shorter.

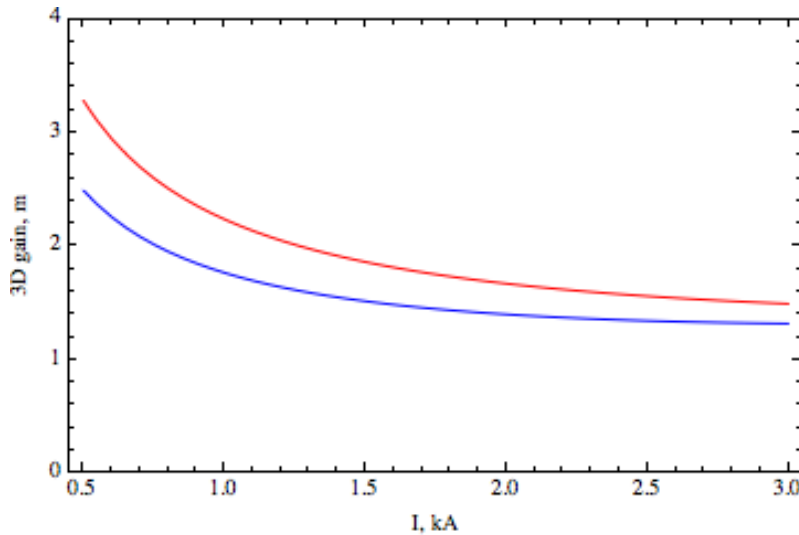


Fig. 5. The 3D FEL power gain length as function of the electron beam peak current for the helical (blue curve) and planar (red curve) undulators.

One can see that the desirable peak current for obtaining small gain length is approximately 2 kA or more. Here we propose reaching this current using the enhanced SASE (ESASE) technique [6].

The schematic of the proposed FEL is shown in Figure 6. Here, the electron beam energy is modulated with an optical laser with the wavelength λ_L ($\omega_L = 2\pi c/\lambda_L$) in the undulator-modulator U0 to have a series of equally spaced femtosecond-scale current spikes after the downstream magnetic chicane. Due to the current-enhanced FEL gain in the following undulator U1, the resulting radiation output is a train of femtosecond x-ray pulses. At the same time, the radiation spectrum is a typical SASE spectrum. After U1, the electron bunch passes the second magnetic chicane, which destroys microbunching at the radiation wavelength and enhances bunching at the optical wavelength. The chicane also delays the arrival time of the electron bunch in undulator U2 such that it appears there simultaneously with the monochromatic wave produced by the forward Bragg scattering of the upstream SASE radiation in the diamond monochromator located in the middle of the magnetic chicane between undulators U1 and U2. This monochromatic wave follows each SASE pulse transmitted through the diamond crystal and typically extends over 20-40 fs. Thus, the monochromatic waves produced by femtosecond

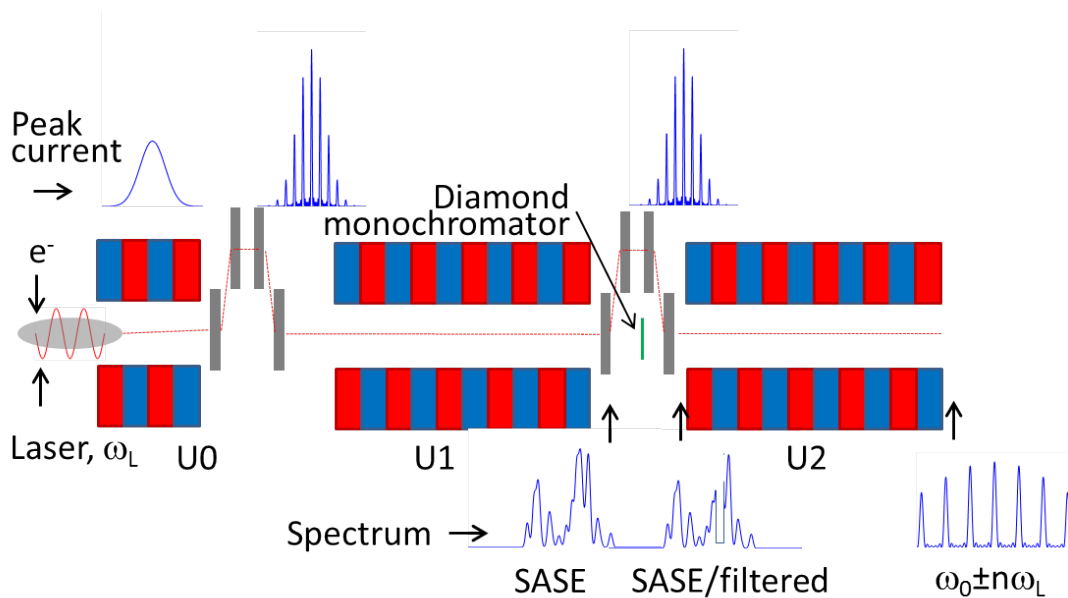


Fig. 6. A schematic of the FEL for self-seeding operation at ~ 5 -keV photon energy using the current-enhanced SASE technique (ESASE) and a diamond monochromator.

SASE pulses (separated by just a few femtoseconds) combine together to create extending regions of temporal coherence with durations of the order of 20 - 40 fs. It is therefore important that the chicane delay is fine tuned to provide interleaving of the electron spikes and SASE spikes as shown in Figure 7. In this case, the broadband high-intensity SASE radiation interacts in U2 with low-intensity regions of the electron bunch, while the low-intensity monochromatic “wake” interacts with the high-intensity regions (spikes) of the electron bunch.

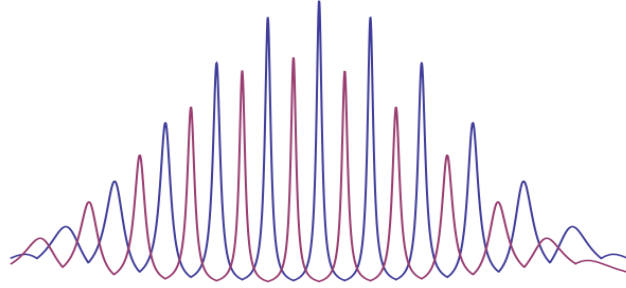


Fig. 7. The electron bunch “train” (blue peaks) and SASE radiation coming from U1 and passing through the diamond crystal (red peaks).

In the subsequent FEL amplification in undulator U2, the radiation field from the ESASE current spikes is coupled together by this monochromatic wave [7]. The FEL will amplify the spectral modes that are within the FEL gain bandwidth, and the resulting frequency-comb mode spacing equals the laser frequency ω_L . Thus, the number of “teeth” in the frequency comb will be proportional to the ratio of the FEL bandwidth to the laser frequency ω_L , while the width of any spectral “tooth” is inversely proportional to the total temporal duration of the pulse train.

In the next step we define the relative amplitude of energy modulation in U0 as $B = \Delta E / \sigma_E$ and calculate the 3D power gain length for various B as a function of the average beta-function β in the undulator. We note that using B is rather convenient since, according to empirical formulas in [6], it characterizes both the spike’s peak current and the energy spread. Figure 8 shows the result.

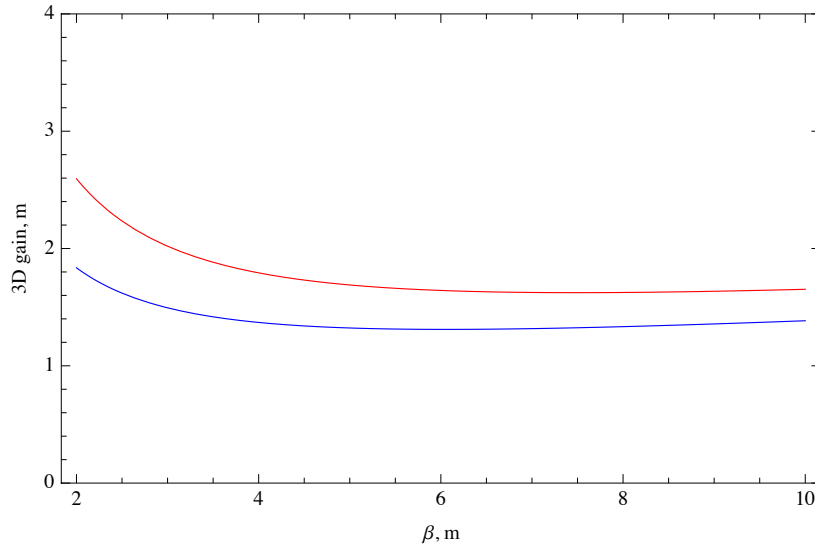


Fig. 8. The 3D FEL power gain length as a function of the average beta-function in the undulator calculated for $B = 4$ for helical (blue curve) and planar (red curve) undulators.

The number of undulator periods in the power gain length that we obtain from Figure 8 for $B=4$ and $\beta = 10$ m is $M_g=154$ for a helical undulator and $M_g=138$ for a planar undulator. Thus, it is expected that the slippage distance over 16 power gain lengths required for the FEL saturation will be:

$$\delta z = 16M_g \lambda_1 = \begin{cases} 0.61 \mu m & \text{helical} \\ 0.55 \mu m & \text{planar} \end{cases} . \quad (9)$$

The FWHM of each electron spike is approximately equal to $\Delta z = \lambda_L / 2B$. Thus, in order for the electron spike to be wider than the slippage length, i.e., $\Delta z \geq \delta z$, the laser wavelength should be [6]:

$$\lambda_L \geq 2B\delta z = \begin{cases} 4.9 \mu m & \text{helical} \\ 4.4 \mu m & \text{planar} \end{cases} . \quad (10)$$

Finally, we estimate peak x-ray power for 5-keV photons at saturation using the empirical formula for the 3D FEL amplification process from Ref. [8]:

$$\begin{aligned} P_{\text{peak}} &\approx 1.8 \text{ GW} && \text{helical} \\ P_{\text{peak}} &\approx 2.4 \text{ GW} && \text{planar} . \end{aligned} \quad (11)$$

Thus, the average power over the entire set of x-ray spikes with a duty factor of $\sim 1/(2B) = 1/8$ is ~ 210 MW for the helical undulator and ~ 300 MW for the planar undulator.

In order for the FEL scheme to operate as described, efficiency of seeding of the FEL in the U2 undulator by the monochromatic “wake” should be higher than efficiency of seeding by the SASE light. Interleaving of the SASE spikes and the electron current spikes ensures that SASE light interacts with electrons only in the regions with a low peak current. However, since the SASE light is more powerful than the monochromatic “wake” by many orders of magnitude, it is not entirely obvious that interleaving is sufficient to bring the FEL amplification in these regions to a level that is below the FEL amplification in the regions with high peak current seeded by the monochromatic “wake.” We also note that the slice energy spread in the low-current regions is smaller than the slice energy spread in the high-current regions. Nevertheless, we estimate that the FEL gain length in the low-current regions should be longer than that in the high-current regions by a factor of ~ 3 . Having these uncertainties, we believe that more accurate results and a better understanding of the interplay of the FEL processes along the electron bunch in U2 should be obtained from computer simulations.

V. Conclusion

Based on preliminary considerations, we conclude that the FEL providing photons in the energy range from 4 keV to 5 keV will need a 2.7-GeV electron beam in the case of the helical undulator with a period of 0.9 cm, and a 3-GeV beam in the case of the planar undulator with a period of 1.2 cm. In the ESASE mode, where the electron peak current is enhanced to approximately 2 kA, the 3D gain power length for 5-keV photons is equal to approximately 1.4 m, and the total length of the undulator needed to reach saturation is equal to approximately 22 m in the case of the helical undulator; the corresponding values for a planar undulator are 1.6 m and 26 m. Two undulators are needed for a self-seeding operation using the diamond crystal between them.

Acknowledgments

The author benefitted from discussions with Paul Emma and Marco Venturini and other members of the NGLS team. The author thanks John Byrd and John Corlett for the support during his stay at LBNL. This work was supported by the U. S. Department of Energy, Office of Science, under Contract No. DE-AC02-06CH11357.

VI. References

- [1] See website: <http://www.aps.anl.gov/Upgrade/News/first-light.html>
- [2] J. Bahrtdt, Y. Ivanyushenkov, Journal of Physics: Conference Series (JPCS) 425, 032001 (2013).
- [3] Y. Ivanyushenkov provided fitting coefficients for Eq. (1).
- [4] J. Murphy and C. Pellegrini in *Laser Handbook*, vol. 6, p. 9, Elsevier Sci. & Tech. (1990).
- [5] M. Xie, Nucl. Instrum. Methods A 445, 59 (2000).
- [6] A. A. Zholents, Phys. Rev. ST Accel. Beams 8, 040701 (2005).
- [7] N. R. Thompson and B. W. J. McNeil, Phys. Rev. Lett. 100, 203901 (2008).
- [8] K.-J. Kim and M. Xie, Nucl. Instrum. Methods A 331(1-3), 359 (1993).